AGARD

ADVISORY GROUP FOR AEROSPACE RESEARCH & DEVELOPMENT

7 RUE ANCELLE 92200 NEUILLY SUR SEINE FRANCE

Paper Reprinted from
Conference Proceedings No. 242
Performance Prediction Methods

NORTH ATLANTIC TREATY ORGANIZATION

FLIGHT TEST VERIFICATION OF F-15 PERFORMANCE PREDICTIONS

J. M. Abercrombie
Section Chief Technology-Aerodynamics
Aerodynamics Department
McDonnell Aircraft Company,
A Division of McDonnell Douglas Corporation

Summary

The prediction of the performance characteristics of the F-15 Eagle was based primarily on data obtained in an extensive wind tunnel test program. This test program was designed to determine the basic lift and drag characteristics for all flight conditions. In addition, the effects of engine operating conditions as reflected in inlet mass flow and engine nozzle geometry and jet plume characteristics were carefully measured. Inlet performance model tests served to provide accurate definition of recovery characteristics for calculation of net propulsive forces.

This paper discusses the test techniques and the methods used to adjust the wind tunnel results to predicted flight performance. A description of the flight test program for performance qualification is also included. Selected comparisons of predicted performance with flight test results are presented. Assessment of the performance prediction methods used, based on the degree of verification available from flight test data, is included.

The results of the F-15 performance flight testing have proven that with sufficiently sophisticated wind tunnel models and thorough test techniques, satisfactory performance predictions can be made. There are, however, areas where improvement in performance prediction is desirable - notably in the prediction of transonic zero-lift pitching moment and of high angle of attack lift characteristics.

1. Introduction

The design requirements imposed on the F-15 Air Superiority Fighter from its inception encompassed a very broad range of Mach number, altitude, and load factor conditions. As a consequence, and because of the very stringent performance requirements, performance predictions were based primarily on a very thorough wind tunnel test program. This test program was necessary because:

- Analytical procedures which could accurately assess the complexities of the configuration were not available.
- Analytical methods were not adequate to handle mixed subsonic/supersonic flows with local shocks and separated regions where viscous effects are strong.
- Primary emphasis was placed on maximizing maneuvering performance at high angle of attack instead of cruise and maximum speed performance which was the norm prior to the F-15 program.

The F-15 Eagle configuration (Figure 1) evolved through one of the most extensive wind tunnel test programs ever conducted for a fighter aircraft. For example, Figure 2 shows the wind tunnel test hours utilized for aerodynamic and propulsion tests on the Eagle compared to previous McDonnell designed fighter aircraft up to the time of first flight. More than 22,000 test hours were accomplished on the F-15 - over four times the number of hours for the F-4 Phantom. Although Figure 2 may imply that future wind tunnel test requirements will increase to extreme levels, the experience and confidence gained in the F-15 development testing should actually reduce the scope of testing to an intermediate level, at least for conventional aircraft. Figure 3 presents a time history of the aerodynamic and propulsion testing accomplished on the F-15. It may be seen that by July 1968, approximately one year before proposal submittal, 2000 hours of wind tunnel test hours had been expended generating design data specifically for the F-15 configuration. At proposal submittal, tunnel testing had grown to more than 10,000 hours, and at contract award, nearly 13,000 hours had been accumulated. These early tests provided data required for studies leading to definition of the more significant aerodynamic/propulsion system features of the F-15 configuration:

- A moderate taper, aspect ratio 3.0 wing combining both conventional and conical camber with simple trailing edge flaps and ailerons.
- Twin vertical tails mounted on aft tail booms.
- An overhead, three ramp, two-dimensional external compression inlet (Figure 4). Variable capture area and near-optimum alignment of the inlet with the incoming airflow for a wide range of angles of attack are provided by pivoting the entire upper cowl and compression ramp. Cowl motion is scheduled automatically as a function of Mach number, angle of attack, and total temperature.
- A nozzle/afterbody configuration characterized by closely spaced convergent-divergent nozzles.

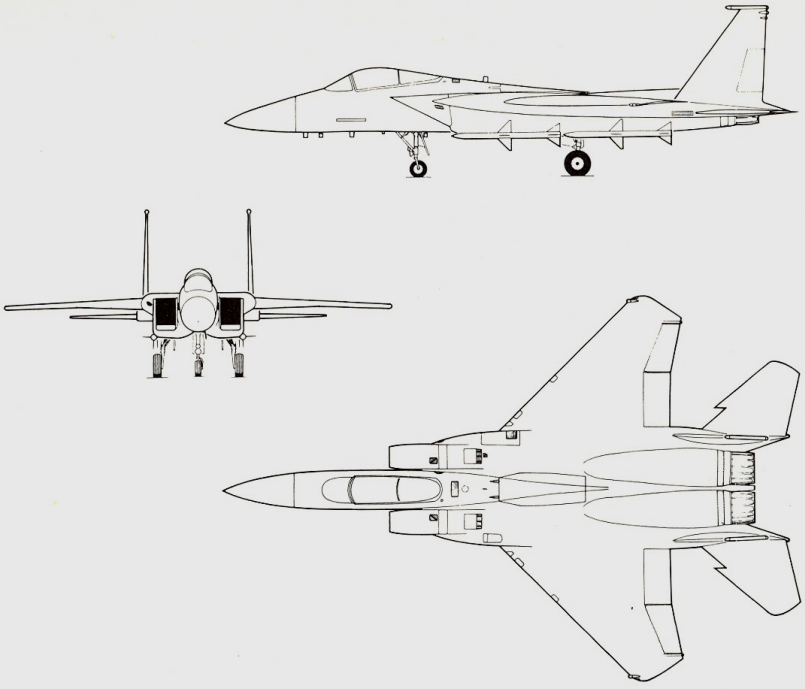

FIGURE 1
GENERAL ARRANGEMENT
MODEL F-15A

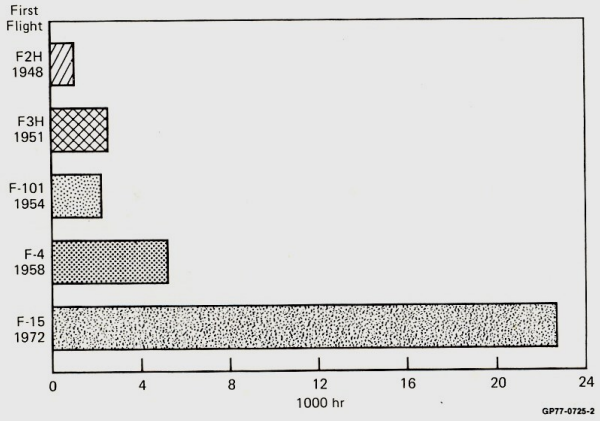

FIGURE 2
WIND TUNNEL TEST HOURS TO FIRST FLIGHT

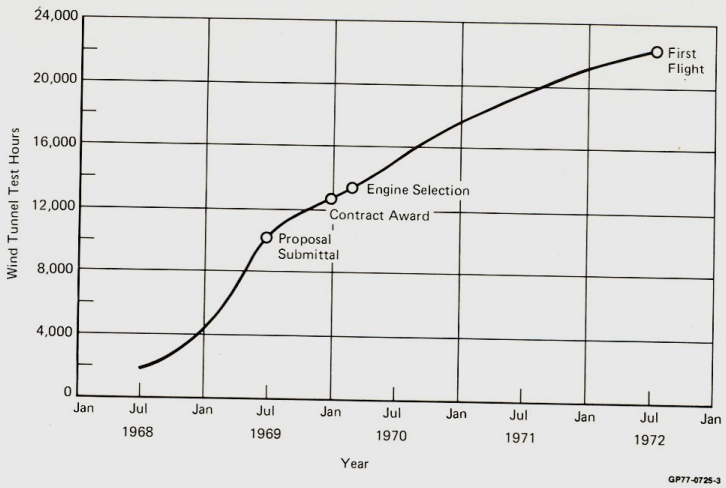

FIGURE 3
AERODYNAMIC AND PROPULSION WIND TUNNEL TESTING

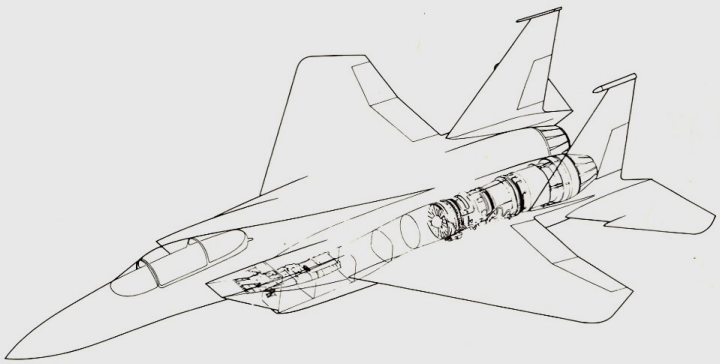

FIGURE 4
INLET/ENGINE INSTALLATION

The wind tunnel testing following contract award was devoted to exploration of potential design improvements and to the acquisition of data to refine and substantiate the estimated performance. These efforts are more fully discussed in Reference 1.

Performance flight testing conducted by MCAIR utilized two aircraft, with the early flights made with pre-production propulsion system configurations. The results of the early flights were used primarily for refinement of engine/inlet controls and schedules. Later, with the production configuration, thirty-five flights were made to formally qualify the aircraft performance.

This paper discusses the wind tunnel test models and techniques used on the F-15, the thrust/drag accounting system employed, and the methods used to estimate full-scale drag characteristics. A description of the flight test program is included, and the techniques used for performance verification are addressed. Comparisons of predicted characteristics to those determined in flight are shown. Areas where improvements in performance prediction are desirable are also discussed.

2. Wind Tunnel Tests

Five sub-scale wind tunnel models were tested for refining the F-15 configuration and establishing the predicted performance. General model descriptions are presented below.

7.5 Percent Sting Mounted Model - The 7.5 percent sting mounted model was a complete configuration model incorporating an operating inlet (Figure 5), inlet ramp bleeds, throat slot bleed and bypass system, and remotely controlled cowls/ramps. All control surfaces were functional. The aft-entry sting required distortion of the afterbody mold lines as illustrated in Figure 6. Inlet duct mass flow was controlled with different exit mass-flow chokes.

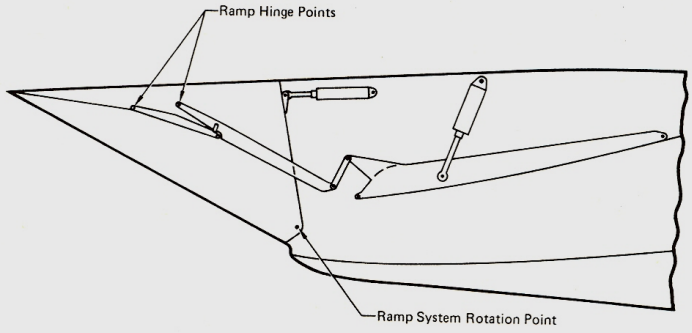

FIGURE 5
7.5% MODEL INLET CONFIGURATION

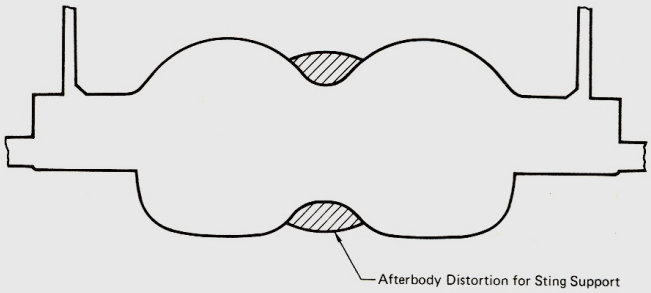

FIGURE 6
AFT ENTRY STING DISTORTION

The entire model was metric with forces and moments measured by a six-component strain gauge balance.

4.7 Percent Sting Mounted Model - The 4.7 percent sting mounted model duplicated the geometry of the 7.5 percent scale model including the sting distortion. Rather than completely functional inlets, however, the 4.7 percent model employed nominal inlet geometry - one configuration representing typical subsonic conditions (cowl leading edge down) with the other (cowl upper surface faired into the nacelle) representative of supersonic conditions.

As in the case of the 7.5 percent model, a six-component balance was used for force and moment measurement.

4.7 Percent Strut Mounted Model - The 4.7 percent strut mounted model was identical to the previously discussed sting-mounted model but with the added capability of being mounted either with a rear entry distorted sting or a single, lower centerline blade support. When strut mounted, the afterbody contours were identical to those of the actual aircraft.

16.7 Percent Inlet Performance Model - The 16.7 percent inlet performance model was a partial configuration consisting of the forward fuselage assembly (extending well aft of the inlets), an inlet assembly, and the required internal duct simulation. The left-hand inlet assembly included the three compression ramps and the diffuser ramp interconnected and remotely controlled to the desired positions as for the 7.5 percent model.

The boundary layer bleed systems consisted of the second and third ramp porous surfaces, throat slot bleed, and inboard and outboard sideplate bleeds. The throat slot also acted as the inlet bypass system for inlet/engine matching. The boundary layer diverter (whose height could be adjusted) included a scaled inlet for the environmental control system (ECS). The model also included an ECS bleed flow plenum around the inlet duct immediately forward of the engine compressor face station. All mass rates of flow were remotely controlled with mass flow chokes.

Primary model instrumentation consists of 246 steady state and 69 high frequency-response pressure sensors including 48 each at the compressor face rake for total pressure, and a total of 16 static pressure sensors at the compressor face.

4.7 Percent Jet Exit Model - The 4.7 percent jet exit model, shown in Figure 7, consisted of a non-metric forward portion simulating the aircraft nose and wing, with the inlets faired from the nose. High pressure external air was introduced through the strut mounting assembly. Special tests were conducted to ascertain the effects of the inlet fairing. These tests showed that there were only slight effects of the fair - ings on the jet plume increment. The metric aft one-third of the model simulated the contours of the nozzle shrouds and tail booms, deflectable horizontal tails, and vertical tails with deflectable rudders.

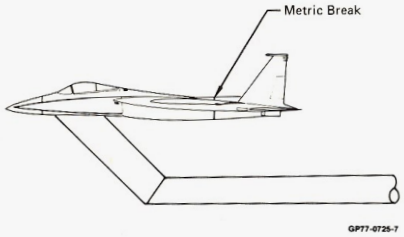

FIGURE 7
4.7% JET EXIT MODEL

Thrust and drag data were obtained with a tandem balance arrangement wherein the main (three-component) balance measured the thrust while the second (six-component) balance measured the afterbody forces and moments.

Thrust/Drag Accounting System

A refined thrust/drag accounting system was devised for use in the F-15 wind tunnel test analyses for the purpose of:

- Avoiding potential errors due to double accounting and/or omission of some drag element.
- Substantiation of total system performance with a minimum of analytical corrections.

As a result, a high level of performance substantiation was achieved.

Figure 8 illustrates the F-15 thrust/drag accounting system and the wind tunnel models used for its implementation. Basic lift and drag characteristics were obtained with the 7.5 percent scale model previously described with its fully operating inlet, aft-entry sting, and the associated distortion of the afterbody mold lines. The inlet mass flow ratio was selected to be as close as possible to the maximum engine operating condition which was selected for the aerodynamic reference point. (Drag variations due to other mass flow ratios were obtained with various exit chokes, and these data were used to adjust the net propulsive force for other operating conditions).

Corrections for sting interference and afterbody distortion were determined from the 4.7 percent scale strut mounted model. In addition, nozzle position effects (unaugmented and maximum afterburner) were measured on this model. High angle of attack (from about 10° to 35°) data were based on the aft entry sting mounted 4.7 percent scale model data.

Finally, analytical estimates of roughness and protuberance drag and of full scale Reynolds number effects were applied to the wind tunnel aerodynamic data.

Net propulsive force prediction utilized the two remaining wind tunnel models: the 4.7 percent scale jet effects model and the 16.7 percent scale inlet performance model. The inlet performance models were used to establish inlet recovery characteristics. Additional corrections for nozzle performance, power extraction, compressor bleed, and leakage were applied to the net propulsive force data.

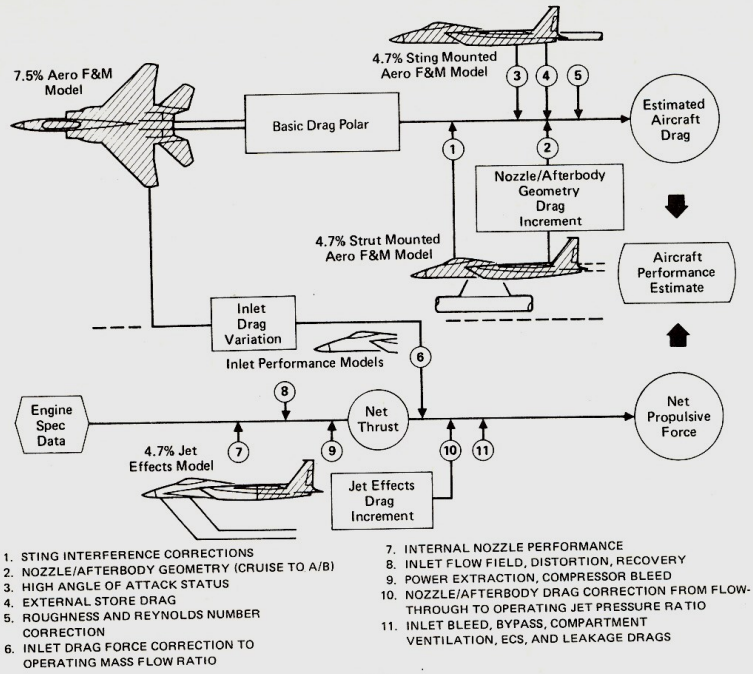

FIGURE 8
F-15 THRUST DRAG ACCOUNTING SYSTEM

The 4.7 percent scale jet effects model yielded corrections to account for jet plume effects at aircraft operating conditions versus the 4.7 percent scale strut mounted model flow-through jet characteristics. These jet induced corrections were also applied to the net propulsive force.

The relative importance of separate elements of the thrust/drag accounting system of Figure 8 are presented in Figures 9 and 10. The drag analysis of Figure 9 is presented for a constant lift coefficient of 0.3 for the maximum afterburner nozzle configuration. Note that the sting and distortion increment (increase) amounts to about three-percent of the subsonic drag and one to four percent of the supersonic drag measured on the 7.5 percent scale aft entry sting supported model, while the analytically determined correction for roughness and Reynolds number (corresponding to 30,000 feet (9144m) altitude) is on the order of 10 percent subsonically and four percent at supersonic conditions. The net propulsive force analysis of Figure 10 is also presented for maximum afterburner, standard day, 30,000 feet conditions. As in the case of the drag analysis, these data illustrate relative insensitivity to any single element of the thrust/drag accounting system.

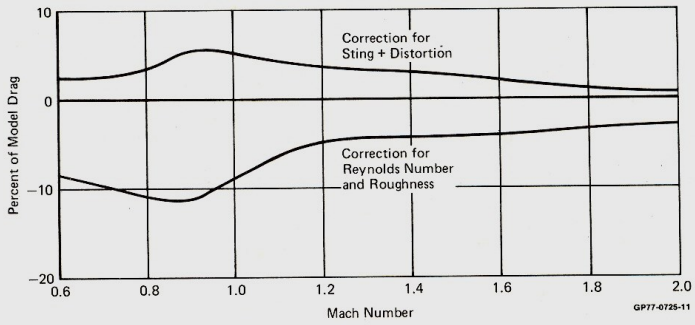

FIGURE 9
WIND TUNNEL TO FULL SCALE CORRECTIONS
$C_L = 0.3$ h = 30,000 Ft. (9,144 m)

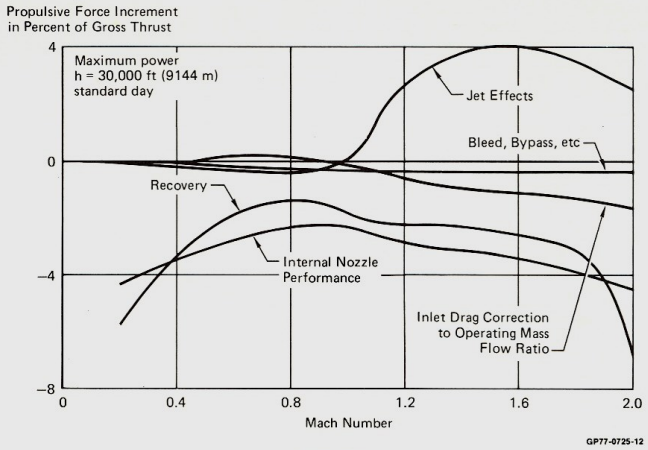

FIGURE 10
PROPULSIVE FORCE INCREMENTS

3. Flight Verification of Predicted Performance

Two of the 13 aircraft used in the contractor flight test program were devoted primarily to propulsion and performance testing. Aircraft No. 2 was used for the early development and refinement of the propulsion system control schedules, engine/inlet compatibility evaluations, and for determining aircraft performance capabilities with the pre-production engines. Details of these early tests are described in Reference 2. Data for formal qualification of performance with the production engines was obtained, for the most part, with Aircraft No. 9. Figure 11 shows the extent of the flight envelope for which quantitative performance data were obtained for formal qualification. These tests were devoted mainly to evaluating the performance at elevated load factors, acceleration to the extremes of the flight envelope, and subsonic cruise. In addition, supporting data were obtained at other portions of the flight envelope with the flying qualities (No. 1), loads (No. 4), and high angle of attack (No. 8) test aircraft.

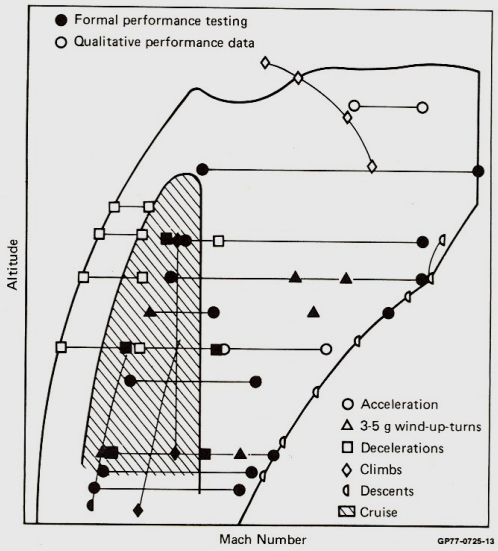

FIGURE 11
PERFORMANCE FLIGHT TESTING

The primary instrumentation used to establish engine performance characteristics, illustrated in Figure 12, consisted of a 32 probe total pressure rake with thermocouples at the inlet face, fan variable guide vane angle, fan speed, a 30 probe total pressure rake at the fan turbine exit, nozzle throat area, fuel flow, and compressor bleed flow. Both the left and the right engines were instrumented.

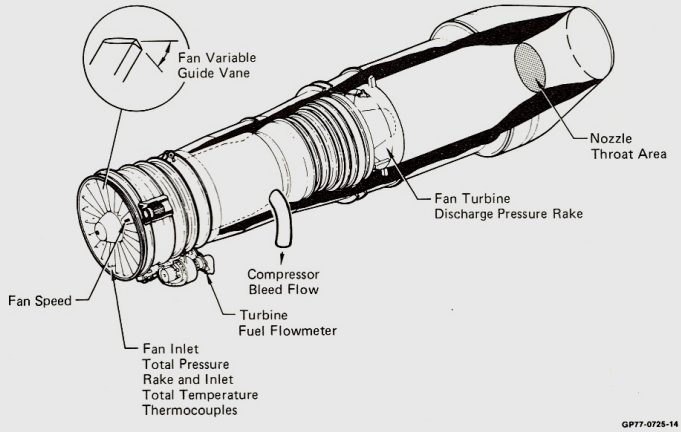

FIGURE 12
ENGINE PERFORMANCE INSTRUMENTATION

The primary aircraft instrumentation for performance evaluation consisted of the usual air data (Mach number, altitude, temperature) in addition to angle of attack, flight path acceleration, fuel state for each of the six fuel tanks, inlet ramp angles, and body angular rates as shown in Figure 13.

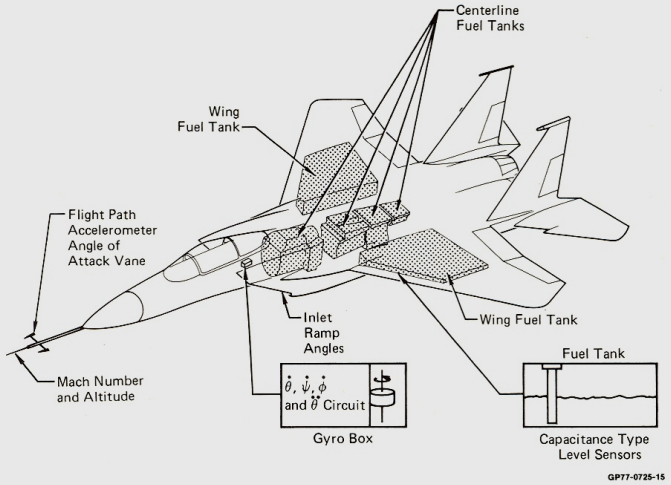

FIGURE 13
AIRCRAFT PERFORMANCE INSTRUMENTATION

Back-up measurands (e.g. body axis accelerometers) were available for data reduction use in the event of instrumentation malfunctions. However, it was rarely necessary to resort to their use.

With these data, it was possible to correct test day conditions (temperature, gross weight, center of gravity location, etc.) to standard conditions as well as to separate the installed engine thrust. Figure 14 illustrates the steps which were undertaken in this procedure for specific excess power, P_S, computation. The data reduction program utilized aerodynamic tables describing the wind tunnel predicted characteristics including the effect of center of gravity location and Reynolds number variations. These were used to provide small corrections for reduction to standard conditions. The propulsion subroutine made use of two programs: the In-Flight Thrust program and the Engine Simulation program. These programs were developed from extensive altitude chamber engine testing with calibrated engine parameters. Test day gross thrust and ram drag were calculated with the In-Flight thrust program. Iteration between the Engine Simulation and Inlet Simulation programs using the measured inlet recovery was employed to arrive at thrust levels predicted for both standard and test day conditions, and increments were used for standardization purposes. From these calculations, not only was the standardized performance determined, but also the lift, drag, and net propulsive force were standardized.

$$P_{S_{st'd}} = \left(P_{S_{test}} + \Delta P_{S_V} + \Delta P_{S_F} + \Delta P_{S_D}\right)\frac{W_T}{W_S}$$

$$\Delta P_{S_V} = \left(\frac{V_S}{V_T} - 1\right)P_{S_{test}}$$

$$\Delta P_{S_F} = \left(\frac{F_{N_{P_S}} - F_{N_{P_T}}}{W_T}\right)V_S$$

$$\Delta P_{S_D} = \left(\frac{D'_T - D'_S}{W_T}\right)V_S$$

$P_{S_{st'd}}$ = P_S Standardized to Desired (Target) Atmosphere, Flight, Weight, Center of Gravity Conditions

$P_{S_{test}}$ = Measured P_S at Test Conditions

W_T = Test gross weight
W_S = Target gross weight
V_T = Test velocity
V_S = Target velocity

$F_{N_{P_T}}$ = Predicted net propulsive force at test conditions
$F_{N_{P_S}}$ = Predicted net propulsive force at st'd day, target conditions
D'_T = Predicted drag at test conditions
D'_S = Predicted drag at st'd day, target conditions

GP77-0725-25

FIGURE 14
FLIGHT TEST DATA REDUCTION
Specific Excess Power - P_S

To accomplish this standardization and facilitate correlation, corrections were applied to account for instrument calibration, non-steady flight, gross weight and center of gravity differences and non-standard atmosphere conditions. The flight path accelerometer data were adjusted to account for any mechanical misalignment and upwash determined by calibration of the nose boom in the wind tunnel as well as for angular rates and pitch acceleration. Net propulsive force was computed using the In-Flight Thrust program. The lift and drag coefficient data were then corrected for Reynolds number effects and center-of-gravity location. Predicted P_S differences between test and standard day conditions were computed; additional increments were calculated to account for velocity, weight, and predicted drag differences between test and standard conditions; and the total were used to adjust the test day P_S to arrive at standardized performance.

For all test points, every attempt was made to fly the aircraft as close as possible to the target conditions to avoid the need for large data reduction corrections. In the event a specified magnitude of correction was exceeded (based on the magnitude of correction relative to the data accuracy), a refly of the test point was required.

Aircraft performance predictions based on the previously discussed wind tunnel test results are reasonably well substantiated insofar as total system performance is concerned. Figure 15 presents comparisons of flight determined specific excess power at 5g normal load factor with the levels which were predicted. It can be seen that within the limits of flight test data accuracy, the agreement is quite satisfactory. Cruise performance comparisons, shown in Figure 16, illustrate that the cruise performance is slightly better than predicted for the high altitude and slightly poorer for the low altitude case. For both conditions, however, the disagreement is very nearly within nominal flight test tolerance.

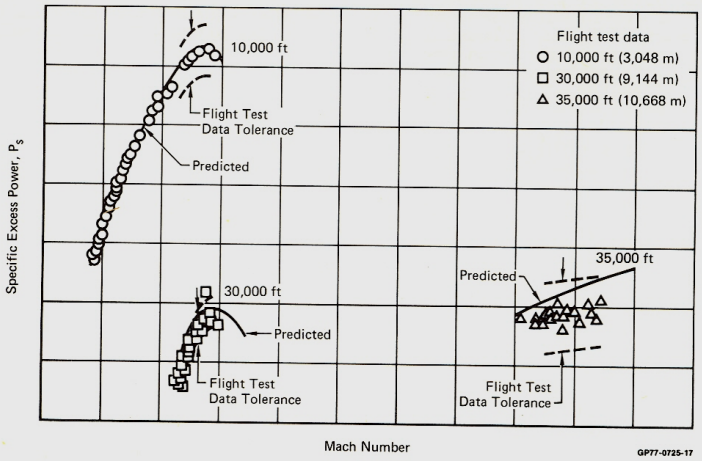

FIGURE 15
SPECIFIC EXCESS POWER COMPARISON
5g Normal Load Factor

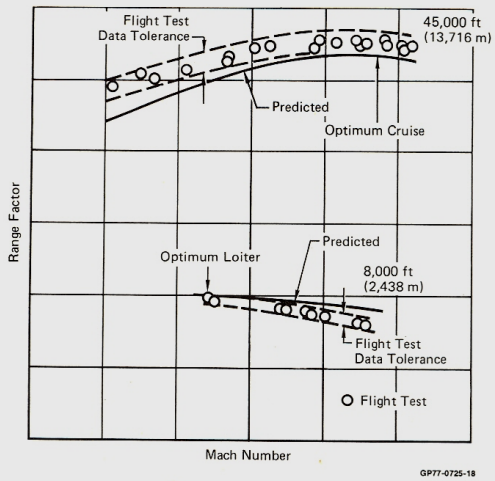

FIGURE 16
CRUISE PERFORMANCE COMPARISON

A further comparison of predicted to actual performance is presented in Figure 17 which summarizes the time-to-climb records established by the F-15 in January and February 1975. Profile development for the six record breaking flights depended on a thorough definition of aircraft lift/drag characteristics and engine performance. Confidence in the predicted performance which was acquired in the early development testing negated the need for special flight tests to generate profile development data. The comparison of predicted and actual time to climb presented in the figure attests to the adequacy of the prediction techniques.

Altitude (meters)	Predicted Time (Predicted Temp) (sec)	Actual Time (sec)	Predicted Time (Test Day Temperature) (sec)
3,000	28.5	27.57	28.5
6,000	39.8	39.33	39.8
9,000	49.3	48.86	49.3
12,000	60.0	59.38	60.0
15,000	79.9	77.04	79.9
20,000	129.2	122.94	123.7
25,000	177.4	161.02	161.2
30,000	226.4	207.80	206.2

GP77-0725-26

FIGURE 17
TIME-TO-CLIMB RECORD SUMMARY

Lift and drag coefficient values extracted from the flight test results are compared to predicted levels in Figures 18 through 20. Figure 18 presents the same condition as was addressed in Figure 9 (30,000 feet, C_L = 0.3) while Figures 19 and 20 show complete drag polars for both a subsonic and a supersonic Mach number. Although flight test data scatter is evident, the agreement between predicted and actual drag is satisfactory. There is, however, some disagreement in polar shape at the supersonic condition at the lower C_L values. This phenomenon, discussed in more detail in Reference 1, resulted from a more positive (airplane nose-up) pitching moment for the actual aircraft than predicted from wind tunnel results (Figure 21). As a consequence, at low lift coefficients, the horizontal tail was required to operate in a less favorable portion of the tail drag polar, resulting in increased aircraft drag. To alleviate this problem, the inlet ramp angle schedules were revised based on the flight derived Cm_o to provide more leading edge down deflection in the transonic region. This resulted in reducing Cm_o to a less positive value thereby allowing the horizontal tail to trim at a lower drag level. Flight testing with the revised ramp schedule verified the expected effects, and the low lift coefficient performance was restored to the desired levels. No systematic exploration of the pitching moment discrepancy between wind tunnel and flight has been accomplished; however, it would appear worthwhile to pursue such a task for the purpose of increasing confidence in performance prediction.

An additional area which merits further investigation is in the high angle of attack region. Figure 22 compares the predicted lift curve with that actually obtained in flight. It will be noted that, based on wind tunnel data, a control limited maximum lift coefficient of 1.32 occurring at 30 to 35 degrees angle of attack was anticipated. The actual aircraft, however, achieved a CL_{max} of 1.6 at 40 degrees with no apparent differences in wind tunnel/flight longitudinal stability or control power.

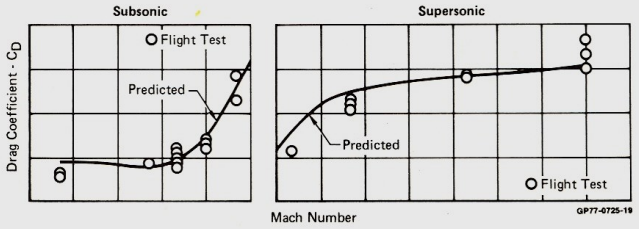

FIGURE 18
DRAG COEFFICIENT COMPARISON
C_L = 0.3 h = 30,000 Ft. (9,144 m)

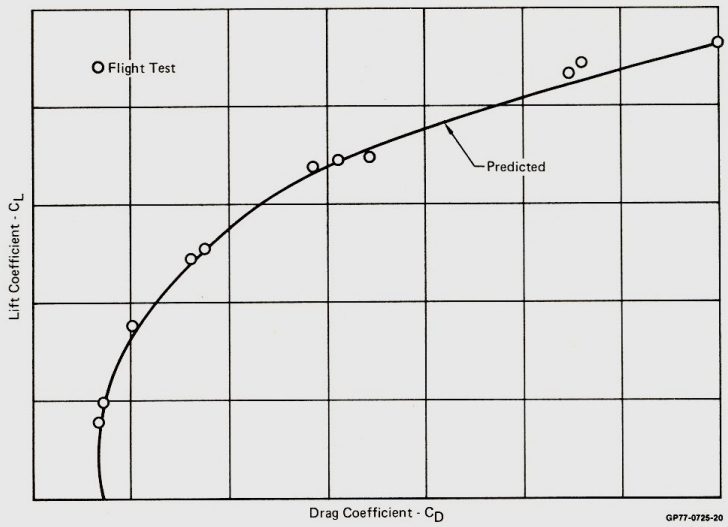

FIGURE 19
DRAG POLAR COMPARISON
SUBSONIC
h = 30,000 Ft. (9,144 m)

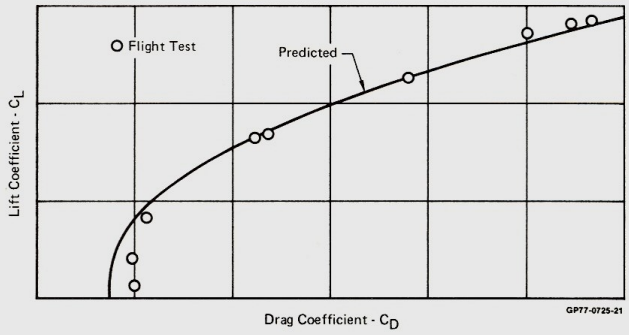

FIGURE 20
DRAG POLAR COMPARISON
SUPERSONIC
h = 30,000 Ft. (9,144 m)

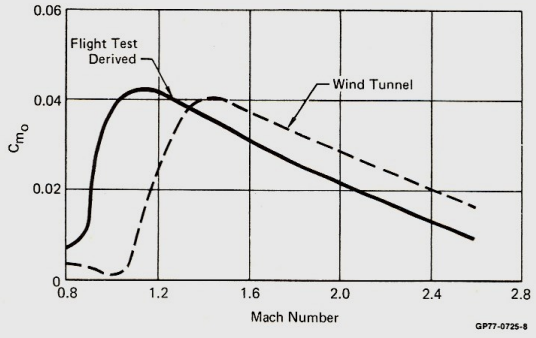

FIGURE 21
ZERO LIFT PITCHING MOMENT COMPARISON

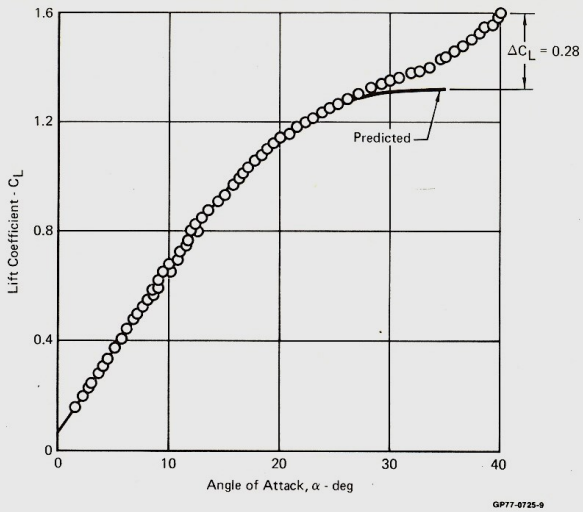

FIGURE 22
COMPARISON OF LIFT CHARACTERISTICS
Subsonic

4. Conclusions

Because of the extensive data base obtained during the wind tunnel development and substantiation testing, a high degree of confidence in predicted aircraft performance was achieved prior to flight evaluation. The results of the F-15 performance flight testing have proven that with sufficiently sophisticated wind tunnel models and with utilization of thorough test techniques, satisfactory performance predictions can be made. This is particularly significant considering the broad range of flight conditions for which performance requirements were imposed.

Performance flight testing was completed with no significant problems. No configuration changes were required as a result of performance deficiencies, and the anticipated performance capability was verified.

References

1. Mello, J.F., "Testing for Design - F-15 Powerplant Integration," AIAA Paper No. 75-002, presented at the AIAA Eleventh Annual Meeting, 24-26 February 1975.

2. Staley, E.J., "F-15 Propulsion Flight Testing Experience," AIAA Paper No. 75-1052, presented at the AIAA 1975 Aircraft Systems and Technology Meeting, 4-7 August 1975.

MDC SENSITIVE

MEMO

241-5673
17 May 78

Subject: MEMO FOR THE RECORD - BASES FOR THE DRAG AND PERFORMANCE DATA PUBLISHED IN NATO AGARD PAPER "FLIGHT TEST VERIFICATION OF F-15 PERFORMANCE PREDICTIONS"

To: J. F. Mello

CC: E. H. Anderson, J. R. Havey, C. H. Mongold

Encl: (1) Substantiation of Drag and Performance Data of AGARD Paper "Flight Test Verification of F-15 Performance Predictions"

1. The subject AGARD paper on F-15 performance prediction/verification was presented at the NATO AGARD Flight Mechanics Panel Specialists Meeting in October 1977. Recent questions regarding the validity of the data presented therein has prompted documentation of the data sources. Enclosure (1) provides such documentation.

Jack M Abercrombie

J. M. Abercrombie
Branch Chief - Technology
Dept. 241, Bldg. 33, Rm 526
Station 23273

JMA:jo

MDC SENSITIVE

SUBSTANTIATION OF DRAG AND PERFORMANCE DATA
OF AGARD PAPER "FLIGHT TEST VERIFICATION OF
F-15 PERFORMANCE PREDICTIONS"

The purpose of the subject paper was to illustrate that F-15 performance predictions, based primarily on wind tunnel test results, were reasonably verified in flight test.

The examples of performance characteristics which were selected for the paper were obtained directly from the F-15 performance qualification report (MDC A3072, Rev. A, 30 Jul 76) with all scales removed from the plots to avoid classification as well as to inhibit the reader from extracting too much information about the F-15's capabilities. The two performance charts used are reproduced on the following page with additional annotations (still unclassified).

The drag coefficient flight data published in the subject paper were extracted from F-9 data using IFTD 1088-1 (SPO Mod 3), as noted. The predicted curves were based on available pre-first-flight wind tunnel data and estimates. As such, adjustments were made to account for the absence of the "knife edge fairings" (which were never flight tested) and for the effects of additional wind tunnel data indicating a revision to the lower C_L drag polar shape. It should be noted that pre-first-flight estimates did not include the effects of the raked wing tips which were incorporated on F-9. However, per Report A0930, the raked wing tip effects were negligible. The drag data which were published in the paper are reproduced on Page 3 with additional annotations defining the scales, Mach number, and power settings.

Memo: 241-5673
Enclosure (1)

PERFORMANCE DATA BASIS

PRINTED FIGURES FROM AGARD PAPER
"FLIGHT TEST VERIFICATION OF F-15
PERFORMANCE PREDICTIONS"

ALL DATA EXTRACTED FROM MDC A3072

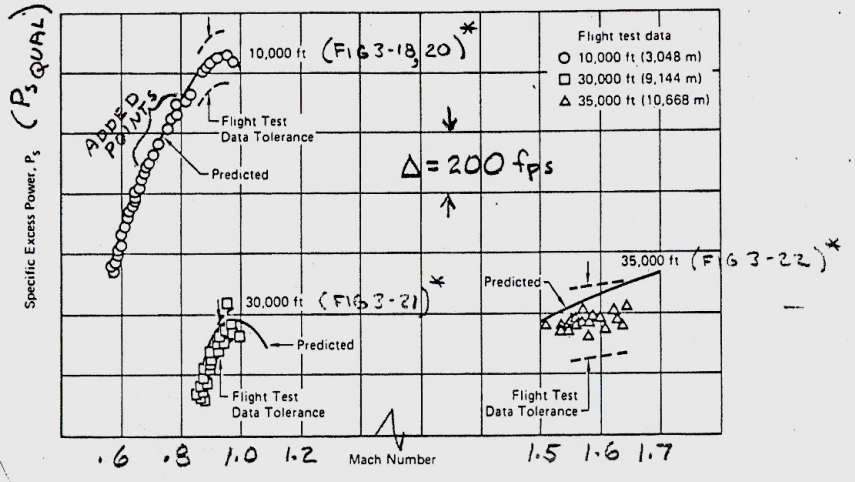

FIGURE 15
SPECIFIC EXCESS POWER COMPARISON
5g Normal Load Factor
Max/Vmax Power

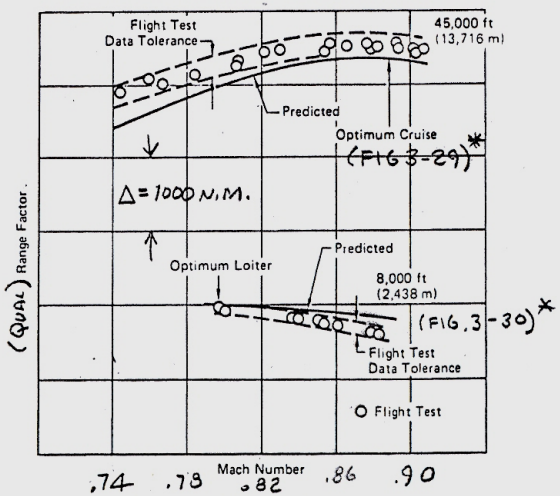

FIGURE 16
CRUISE PERFORMANCE COMPARISON

* REFERS TO MDC A3072 FIGURE NUMBERS

DRAG DATA BASIS

PRINTED FIGURES FROM AGARD PAPER "FLIGHT TEST VERIFICATION OF F-15 PERFORMANCE PREDICTIONS"

FLIGHT TEST DATA FROM CAT. I, F-9 FLIGHTS 122-154, ENGINE S/N 085, 086, AND IN-FLIGHT THRUST DECK 1088-1(SPO MOD 3)

PREDICTED CURVES ARE ESTIMATES PRIOR TO 1ST FLIGHT (RPT A0930) WITH FOLLOWING ADJUSTMENTS

SUBSONIC ~ ADDED 10 COUNTS FOR ABSENCE OF "KNIFE-EDGE" FAIRINGS

SUPERSONIC ~ REVISED LOW C_L POLAR SHAPE BASED ON WIND TUNNEL DATA OBTAINED PRIOR TO FIRST FLIGHT BUT NOT INCORPORATED IN A0930 STATUS.

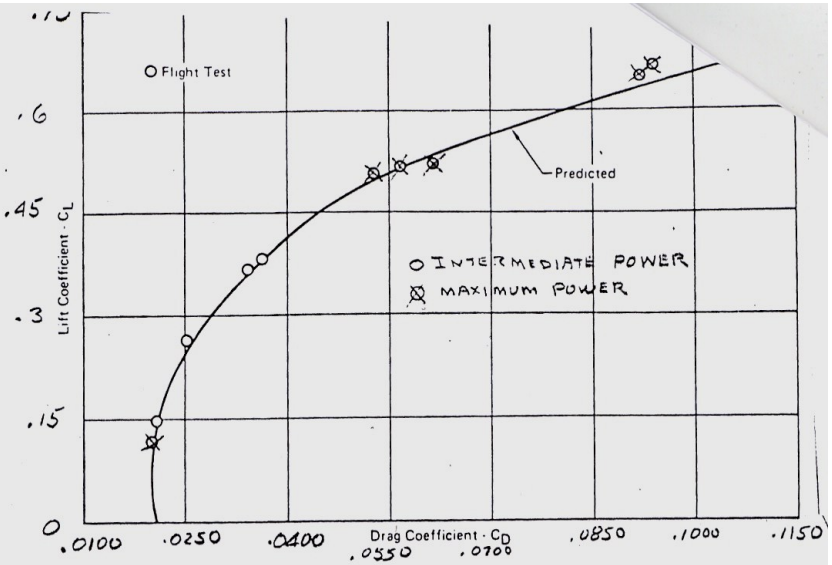

FIGURE 19
DRAG POLAR COMPARISON
SUBSONIC
M = .6
h = 30,000 Ft. (9,144 m)

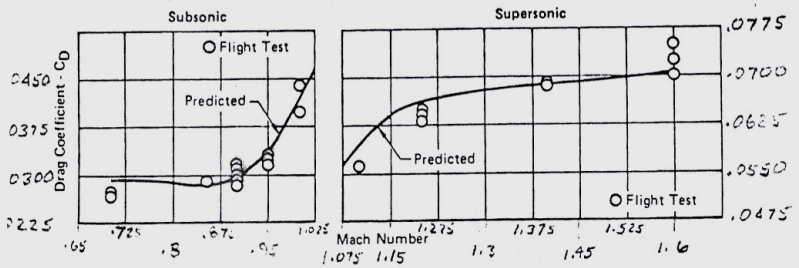

FIGURE 18
DRAG COEFFICIENT COMPARISON
C_L = 0.3 h = 30,000 Ft. (9,144 m)

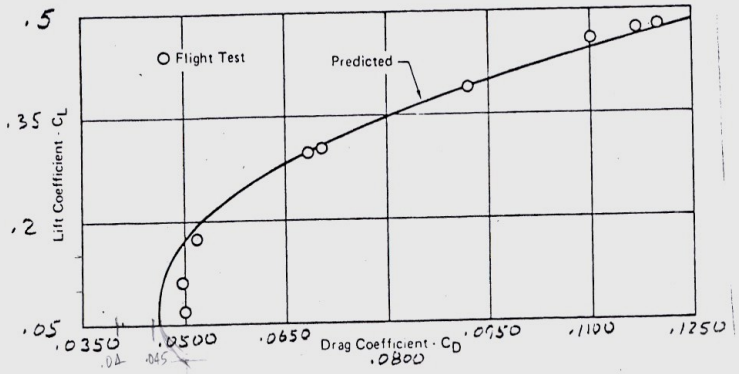

FIGURE 20
DRAG POLAR COMPARISON
SUPERSONIC
M = 1.4
MAX. POWER
h = 30,000 Ft. (9,144 m)